Analysis of Atlantic extratropical storm tracks characteristics in 41 years of ERA5 and CFSR/CFSv2 databases

Article

Accepted Version

It is advisable to refer to the publisher's version if you intend to cite from the work. See Guidance on citing.

To link to this article DOI: http://dx.doi.org/10.1016/j.oceaneng.2020.108111

Publisher: Elsevier

www.reading.ac.uk/centaur

CentAUR

Central Archive at the University of Reading

Reading's research outputs online

Analysis of Atlantic extratropical storm tracks characteristics in 41 years of ERA5 and CFSR/CFSv2

C.B. Gramcianinov[12*], R.M. Campos[1], R. de Camargo[2], K.I. Hodges[3], C. Guedes Soares[1], P.L. da Silva Dias[2]

[1]Centre for Marine Technology and Ocean Engineering (CENTEC), Instituto Superior Técnico, Universidade de Lisboa. Rovisco Pais, 1049-001 Lisboa, Portugal.

[2]Departamento de Ciências Atmosféricas, Instituto de Astronomia, Geofísica e Ciências Atmosféricas, Universidade de São Paulo, Rua do Matão 1226, Cidade Universitária, São Paulo, SP, Brazil.

[3]Department of Meteorology, University of Reading, Reading, United Kingdom.

*Corresponding Author, e-mail address: cbgramcianinov@gmail.com

ABSTRACT: This work aims to analyze and compare ERA5 and CFSR/CFSv2 from 1979 to 2019 with 1-hourly outputs, regarding their ability to reproduce storm tracks and the main characteristics of cyclones at middle and high latitudes in the North Atlantic (NA) and South Atlantic (SA) Oceans. The cyclone tracking was based on relative vorticity at 850 hPa and the intensity is measured using the maximum 10-meter wind speed. The climatology produced for both datasets shows the main characteristics of the NA and SA storm tracks, such as seasonal variability and genesis regions. The use of 1-hourly fields improves tracking in areas with complex terrains, such as the lee of Andes (SA) and Greenland (NA). The differences in cyclone numbers and characteristics between datasets are small. 92.7% and 93.1% of ERA5 cyclones have an identical correspondent storm in CFSR/CFSv2, in the NA and SA respectively. Genesis and lifetime statistics show that CFSR/CFSv2 may present inconsistency between forecast and analysis sequential time-steps. Large differences remain in the intensity distributions, in which the CFSR/CFSv2 presents stronger cyclones than ERA5. Divergences between the datasets decrease when the comparison is made using only CFSv2, particularly in the South Atlantic.

Keywords: Extratropical cyclones; storm tracks; cyclogenesis; South Atlantic Ocean; North Atlantic Ocean; reanalysis.

1. Introduction

Cyclones are key features of the day-to-day weather variability at middle and high latitudes. Storminess is an important risk for offshore structures and ship routing, particularly due to their associated extreme winds and waves (Ponce de León and Guedes Soares, 2012; Vettor and

22 Guedes Soares, 2016; 2017). Safe and profitable engineering operations depend on weather

23 forecasts and metocean statistics, the last being usually produced from reanalysis data produced

24 by operational centers around the world (Campos et al., 2018; 2019). Transient system variability

25 in the extratropics are the contributor to not only errors in wind-wave forecasts but also for

26 problems associated with the representation of topographic and sea surface temperature gradient

27 effects in ocean models (Chelton et al., 2004). Cyclone tracks are usually obtained using 6-

28 hourly data sources, which are necessary to produce reliable cyclone tracks but are insufficient

29 for some ocean engineering problems, such as wave hindcast and forecast models. In this paper

30 cyclone tracks in the Atlantic Ocean from two modern reanalysis datasets are compared, the fifth

31 generation of reanalysis from the European Centre for Medium-Range Weather Forecast

32 (ECMWF; Hersbach and Dee, 2016) (ERA5), and the Climate Forecast System Reanalysis

33 (CFSR; Saha et al., 2011), and Climate Forecast System version 2 (CFSv2; Saha et al., 2014)

34 from the National Center for Environmental Prediction (NCEP). Besides the analysis of these

35 two datasets and the discussion, an important contribution of this work is to produce a cyclone

36 database that can be used to support ocean engineering and coastal hazard estimations, together

37 with an evaluation of the main differences between the two datasets.

38 Automated methods for cyclone identification and tracking have been developed in the past

39 decades, due to the increase of available data produced by Global Circulation Models (GCMs)

40 and reanalyses, led by the improvement of computational resources. These objective methods are

41 based on a Lagrangian approach that generally uses low-level vorticity or surface pressure

42 criteria to identify and track cyclones (e.g., Murray and Simmonds, 1991; Sinclair, 1994;

43 Hodges, 1994; 1995). Since then, a wide set of cyclone climatologies have been produced for the

44 Northern Hemisphere (e.g., Hoskins and Hodges, 2002), Southern Hemisphere (e.g., Jones and

Simmonds 1993; Sinclair 1994; Simmonds and Keay, 2000; Hoskins and Hodges, 2005), North Atlantic (e.g., Pinto et al., 2005; Trigo, 2006; Dacre and Gray, 2009, Grise et al., 2013), and South Atlantic Oceans (e.g., Mendes et al., 2010, Reboita et al., 2010, Gramcianinov et al., 2019). The basic product of the tracking method is the collection of cyclone trajectories within a defined region and period. The spatial statistic distribution of this collection of trajectories defines the storm track position – the preferred location of cyclone propagation.

Following the development of GCMs, the use of analyses and reanalyses was a valuable improvement to the atmosphere and ocean dynamics studies (Parker, 2016). Reanalysis products are based on a model allied to data assimilation, and thus, can provide a complete spatial coverage at a regular resolution. Despite the verification and validation performed by development centers (e.g., Kalnay et al., 1996; Saha et al., 2011; 2014), it is important to evaluate the performance of these datasets for particular applications, such as extratropical and tropical cyclones, and precipitation. Several studies have carried out intercomparisons of storm tracks obtained from different datasets for the whole globe (e.g., Hodges et al., 2003; 2011), Northern Hemisphere (e.g., Raible et al., 2008), North Atlantic sector (e.g., Trigo, 2006) and South Atlantic sector (Reboita et al., 2018; Crespo et al., 2020a). Hodges et al. (2011) compared the storm track distribution and intensity in four reanalysis: the Modern Era Retrospective-Reanalysis for Research and Applications (MERRA; Rienecker et al., 2011), the 25-yr Japan Reanalysis (JRA25; Onogi et al., 2007), the ECMWF Interim Reanalysis (ERA-Interim; Simmons et al. 2007), and the CFSR. They found larger discrepancies between the older and newer products and attributed their findings to the improvement of data assimilation techniques and increase of resolution. According to them, modern reanalysis inter compares better than the older ones for cyclone densities. However, differences remain large between CFSR and ERA-

Interim for cyclones intensities, and also for densities in some regions of the Southern Hemisphere. Stopa and Cheung (2014) evaluated 30 years of wind and wave data from the CFSR and ERA-Interim using altimeter and buoy observations. While ERA-Interim presented lower error metrics, CFSR showed a better performance in the upper percentiles associated with extreme events. The large differences between datasets are generally associated with the failure in the representation of extreme events (e.g., Stopa and Cheung, 2014; Campos et al., 2018). Winds are often underestimated at some locations, mainly in the Southern Hemisphere, due to the lack of observational data (e.g., Stopa and Cheung, 2014). This problem contributes to the misrepresentation of cyclones, particularly the most intense ones, which leads to issues in wind-wave climate hindcast and forecast (e.g., Kumar et al., 2003; Campos and Guedes Soares, 2016; 2017; Bakhtyar et al., 2018; Mattioli et al., 2019; Campos et al., 2019), and storm surge estimations (e.g., Colle et al., 2010; Booth et al., 2016; Sebastian et al., 2019).

Therefore, it is important to evaluate cyclone and storm track characteristics of datasets available at high temporal resolution, since 1-hourly fields are frequently used to support the production of wave hindcasts and forecasts, and energy sector assessments. The main goal of this study is to present and evaluate the Atlantic cyclone climatology for middle and high latitudes that can be used by research and industry applications, since there is a lack of this type of product available (e.g., Dacre et al., 2012), particularly for the South Atlantic Ocean. Therefore, two main questions for this study are: (1) How does the 1-hourly ERA5 and CFSR/CFSv2 cyclone tracks for the Atlantic storm track compare with previously published studies?; (2) What are the main differences between the two datasets regarding the basic cyclone and storm track characteristics? The analysis is focused on the mean characteristics, spatial distribution and intensity of the cyclones, which are important features that control the wind and wave climates.

2. Data and Methods

2.1. Datasets

ERA5 is the latest reanalysis produced by ECMWF, available from the Copernicus Climate Change Service (CS3). This reanalysis has been produced using 4D-Var data assimilation in ECMWF's Integrated Forecast System (IFS), version CY41R2. The atmospheric variables used in this work are on a 31 km (0.28125°) horizontal grid with 1-hourly outputs from 1979 to 2020. ERA5 replaces the ERA-Interim, and benefits from its antecessor's development in model physics, core dynamics and data assimilation. One of the most important innovations of ERA5 is output of hourly analyses that can widely support risk and operational management in diverse sectors, such as renewable energy (e.g., Olauson, 2018). Moreover, Belmonte Rivas and Stoffelen (2019) found that ERA5 surface winds present a 20% improvement relative to ERA-Interim, using ASCAT observations as verification. An overview of the main characteristics of ERA5 and a comparison with ERA-Interim can be found in Hersbach et al. (2018).

The CFSR is the latest version of the NCEP climate reanalysis and covers the period from 1979-March/2011. The reanalysis was produced using a coupled atmosphere–ocean model: the NCEP Global Forecast System (GFS) for the atmosphere and the Geophysical Fluid Dynamics Laboratory Modular Ocean Model version 4 (MOM4) for the ocean (Saha et al., 2010). The CFSv2, the operational descendant of the CFSR, was released in March 2011, and it has been running operationally since then. The CFSR and CFSv2 have a horizontal native resolution of T382 (~38 km) interpolated to a 0.5° x 0.5º grid. Both the reanalysis and analysis are produced originally in 6-hourly intervals, but a 1-hourly time series are also available from some variables and consist of the analysis followed by the sequence of hourly forecasts until the next analysis

114   cycle. The hourly sequence provided might have abrupt changes in atmospheric fields every time

115   when a forecast time-step changes to analysis time-step, since the last is corrected by data

116   assimilation. Despite this eventual inconsistency along the period, it is important to evaluate the

117   hourly data since these products are used for ocean engineering applications. Moreover, it is the

118   only way to compare CFSR/CFSv2 with ERA5 1-hourly data. Differences between products are

119   expected and need to be discussed to support future choices and/or changes.

120

121   **2.2. Cyclone identification and tracking**

122   The cyclones are identified and tracked in both reanalyses using the TRACK program

123   (Hodges, 1994; 1995; 1999) following the pre-processing steps described in Hoskins and Hodges

124   (2002; 2005). The cyclonic features were identified using the relative vorticity, which is

125   computed using the zonal and meridional wind components at 850 hPa in spherical coordinates

126   to avoid latitudinal bias (Sinclair, 1997). Sinclair (1994) highlighted the benefit of using vorticity

127   instead of mean sea level pressure (MSLP) for the detection of cyclones in mid-latitudes, where

128   the surface pressure gradient can be strong so that cyclones appear without a closed isobar. For

129   this reason, the use of vorticity allows the early identification of cyclones that would only be

130   detected by MSLP when intensification occurs or they move to higher latitudes. The vorticity

131   field contains many small scale structures, particularly at the high resolution, which can cause

132   problems during the identification process and tracking on the synoptic scale. To prevent this

133   issue and focus on synoptic scales, the vorticity was spectrally filtered by converting to the

134   spectral representation and truncating to T42, tapering the spectral coefficients to smooth the

135   data. Large-scale atmospheric features were also removed by setting zonal wavenumbers ≤ 5 to

136   zero. Hoskins and Hodges (2002) present more details about the filtering.

137   The cyclonic features are identified by determining the local maxima. In the Southern

138   Hemisphere, where negative vorticity indicates cyclonic circulation, the vorticity fields are first

139   scaled by -1. First, the central position of the cyclonic feature is determined by the grid point

140   maxima that exceed a threshold of 1×10^{-5} s^{-1} (1 cyclonic vorticity unit (CVU)) on a polar

141   stereographic projection. This identification threshold is suitable to capture even weak cyclonic

142   centers in the filtered vorticity field (T42), since it is smoother than the original vorticity one

143   (e.g., Hoskins and Hodges, 2002; 2005). The feature central locations are refined by computing

144   the off-grid maxima using B-spline interpolation and steepest descent maximization and then

145   converted back to spherical coordinates. The tracking is initialized using a nearest neighbors

146   search method. The initial set of tracks is refined by minimizing a cost function for track

147   smoothness, subject to adaptive constraints (Hodges, 1999), that operates both forwards and

148   backward in time. The high time resolution reduces ambiguity during tracking. The displacement

149   constraint applied was 2.0°, except in the tropics (20°N-20°S) where it was set as 0.5°. Due to

150   the large amount of data, the tracking was performed using monthly files. Thus, post-processing

151   was applied to connect tracks between the months, using the same displacements rules described

152   above.

153   Finally, identified systems that are not cyclones were excluded. In this step, cyclonic features,

154   such as thermal lows, mesoscale storms, and some convergence areas were removed by

155   considering only systems that last at least 24 hours and that travel further than 1000 km, such as

156   used by Gramcianinov et al. (2019) for the South Atlantic Ocean. The thresholds are more

157   relaxed than the ones commonly used in North Atlantic storm track studies (e.g., Hoskins and

158   Hodges, 2002; 2005; Hodges et al., 2011; Dacre and Gray, 2009), but it maintains consistency

159   throughout the entire Atlantic. The use of a higher minimum lifetime threshold (e.g., 36h or 48h)

160 would exclude some systems with regional importance (e.g., Gramcianinov et al., 2019; 2020).

161 Gramcianinov et al. (2020) considered cyclones with a minimum of 12h lifetime and 500km

162 displacement, to include short-lived systems that might be important for extreme waves along the

163 Southern Brazilian coast. However, the use of such a low displacement threshold results in

164 including continental lows and non-developed cyclonic systems in the climatology. Figure 1

165 shows the genesis and track densities of cyclonic systems that live at least 24 hours with the total

166 displacement between 500 and 1000 km. In the North Atlantic, 23% (ERA5) and 26%

167 (CFSR/CFSv2) of the cyclonic systems were excluded with the 1000 km (~10º) displacement

168 threshold, while in the South Atlantic they represented a smaller portion of 15% (ERA5) and

169 21% (CFSR/CFSv2). Although these values can be considered important, the track density

170 reveals that systems with small mobility (semi-stationary) are mainly continental and thermal

171 lows generated in complex terrain, and troughs that are generated in frontal zones, without

172 enough forcing for full-development. The genesis densities are smaller when compared to active

173 cyclone genesis regions reported in the literature (e.g., Hoskins and Hodges, 2002; 2005), and

174 the track density is restricted to the generation point revealing the small influence of the systems,

175 which mostly do not reach the ocean.

176 Since the main interest of this work is on cyclones at middle and high latitude, we considered

177 for further analysis storms which pass within the extratropical latitudes of the South Atlantic

178 (85ºS-25ºS, 75ºW-20ºE) and North Atlantic (85ºN-25ºN, 65ºW-0ºE). The selected domains

179 include areas where occurs subtropical cyclones generated both by genuine subtropical genesis

180 and by transition process between tropical and extratropical cyclones (e.g., Guishard et al., 2009;

181 Evans and Braun, 2012; Gozzo et al., 2014). In this way, subtropical cyclones may be included in

182 the set of tracks, since no distinction between subtropical and extratropical cyclones was made in

183 the present work.

184

185 **2.3. Cyclone diagnostics**

186 The statistical analysis consists of information for the tracks, including mean lifetime of

187 cyclones, cyclone speed, and displacement. Standard seasons are used for the entire period

188 (1979-2019): December-February (DJF), March-May (MAM), June-August (JJA), and

189 September-November (SON). Spatial statistics are computed for each reanalysis using the

190 spherical kernel estimator approach, described by Hodges (1996). The differences between track

191 and genesis densities of the two datasets were tested using Monte Carlo significance test

192 (Hodges, 2008) with 1000 samples of the set of tracks for each dataset.

193 Maximum 10-m wind speed is used for the comparison of cyclone intensities. The 10-m wind

194 speed is added to each track by a general search for the maximum value within a 6° radius of

195 cyclone center (Bengtsson et al., 2009). This additional information was used to construct

196 maximum intensity distributions for both ERA5 and CFSR/CFSv2. Moreover, identification of

197 matched tracks between the datasets was made to perform a more direct comparison of the

198 cyclone intensities. A storm was considered to be the same in ERA5 and CFSR/CFSv2 when the

199 mean separation distance between cores was less than 2° (geodesic) and they overlap in time by

200 at 50% of their points. The criteria used here is stricter than the one applied in Hodges et al.

201 (2011), where the minimum mean separation distance was 4°. The choice of a smaller distance

202 agrees with the focus of this work, linked to ocean engineering applications, in which smaller

203 differences in the system position may lead to large biases in the wind and wave fields.

204

3. Results

3.1.Genesis and track densities

Before the direct comparison between storms tracks in each dataset, the climatology of the cyclones is presented, using ERA5 as a reference, to provide an overview of the storm track pattern and genesis variability in the North and South Atlantic Oceans.

3.1.1. North Atlantic

The track and genesis densities in the North Atlantic domain for the entire period, boreal winter (DJF) and summer (JJA) are shown for the ERA5 and CFSR/CFSv2 in Figure 2 and Figure 3. The North Atlantic storm track is represented by the region of maximum track density [> 10 cyclones $(10^{-6}, km^2)^{-1}$ $(month)^{-1}$] extending northeastward, from the East of North American coast to Greenland and North Europe. A northern path of the storm track strengthens in DJF, along the eastern side of Greenland, due to the increase in genesis activity at this location. The genesis density shows four regions favorable to cyclogenesis [> 2 cyclones $(10^{-6}, km^2)^{-1}$ $(month)^{-1}$]: lee of the southern Rockies (35ºN, 102.5ºW), West Atlantic (40ºN, 75ºW), East Atlantic (centered at 50ºN, 25ºW), and in the eastern coast of Greenland.

All genesis regions within the North Atlantic domain are more active during the boreal winter (DJF). However, the genesis region along the eastern North American coast is active all year, being a location with high baroclinicity due to the sea surface temperature gradients provided by the warm Gulf Stream. The surface temperature contrast does not give only conditions to genesis but also to the intensification of pre-existing cyclones and perturbations that come from continent - which may be generated on the lee side of Rockies. Grise et al. (2013) constructed a genesis density distribution using not the first track point of each cyclone but the location where

10

228 storms exceeded the growth rate of 2 CVU per day, and they found a major genesis density along

229 the east coast of North America and less at the Rockies. The genesis region at the lee of the

230 northern Rockies and its consequent storm track density along the continent (e.g., Hoskins and

231 Hodges, 2002) does not appear in Figure 3 because these cyclones dissipate in the northeast

232 portion of the North American continent, outside the North Atlantic domain (Dacre and Gray,

233 2009). The genesis densities along the east Greenland coast are higher in Figure 3 than in some

234 previous studies selecting cyclones that last more than 48 h (e.g., Hoskins and Hodges, 2002;

235 Dacre and Gray, 2009; Grise et al., 2013). Trigo (2006) used the 24h threshold and also obtained

236 a more pronounced genesis density in Greenland.

237

238 *3.1.2. South Atlantic*

239 Figure 4 and Figure 5 show the cyclone track and genesis densities in the South Atlantic for

240 the ERA5 and CFSR/CFSv2, computed for the whole period, as well as divided into austral

241 summer (DJF), and winter (JJA). The main South Atlantic storm track is defined by the high

242 concentration of systems [> 10 cyclones $(10^{-6}, km^2)^{-1}$ (month)$^{-1}$] extending from west to east of

243 the domain, between 40ºS and 55ºS. Furthermore, there is a secondary storm track [> 6 cyclones

244 $(10^{-6}, km^2)^{-1}$ (month)$^{-1}$] that merges with the primary storm track, being considered a

245 subtropical branch. During the austral summer (DJF), the subtropical storm track spreads

246 northward, originating between 30ºS and 35ºS, while during the winter this branch is

247 concentrated in 35ºS. The winter season variability in the South Atlantic storm track is linked to

248 changes in active genesis regions in South America, as is possible to see in the genesis density

249 spatial distribution (Figure 5).

250   The genesis density for all period shows three main regions of active genesis [> 2 cyclones

251   $(10^{-6}, km^2)^{-1}$ (month) $^{-1}$]: in Uruguay (35ºS, 60ºW), Argentinean coast (45ºS, 65ºW), and

252   Antarctic Peninsula (65ºS, 60ºW). Secondary genesis regions exist in the Southeast Brazilian

253   coast (27ºS, 45ºW), and southeast portion of South Atlantic (centered at 45ºS, 10ºW). The former

254   is only pronounced during the austral summer, while the last has more genesis during the winter

255   (e.g., Gramcianinov et al., 2019). In South America, the genesis regions at Uruguay are more

256   active during JJA, while the Argentina's genesis region is more active in DJF. However, the

257   genesis region in Argentina presents a high density of genesis during all year [> 5 cyclones $(10^{-6},$

258   $km^2)^{-1}$ (month) $^{-1}$]. The genesis region in Southeast Brazilian coast and Southeast South Atlantic

259   are more active in CFSR/CFSv2 climatology [> 2 cyclones $(10^{-6}, km^2)^{-1}$ (month) $^{-1}$] than in

260   ERA5.

261   The spatial distribution and seasonal variation presented in Figure 4 and Figure 5 are in

262   agreement with previous studies (e.g., Hoskins and Hodges, 2005; Reboita et al., 2010;

263   Gramcianinov et al., 2019). A more direct comparison can be made with results from

264   Gramcianinov et al. (2019) since the system duration and displacement threshold applied are the

265   same (24 h and 1000 km). They found a slightly more active genesis region in the Southeast

266   Brazilian coast in DJF. Also, the Uruguay genesis region is much more active in the present

267   work, with a genesis density almost 20% larger.

268

269   **3.2. Differences between ERA5 and CFSR/CFSv2 cyclones**

270   Table 1 shows the cyclone annual and seasonal mean frequencies computed for the entire

271   period (1979 to 2011). Such values were also computed for the split period linked to CFSR

272   (1979-March/2011) and CFSv2 (April/2011-2019) separately, to analyze the differences between

273   datasets. In general, ERA5 produces more cyclones than CFSR/CFSv2, which is expected due to

274   the higher resolution of the former. The differences between the two datasets are smaller in the

275   North Atlantic than in the South Atlantic in all cases. In the North Atlantic, the differences in

276   cyclone numbers are between 0.4% and 4.4%, being the lowest and largest differences detected

277   in MAM and JJA respectively. The period of JJA is the only season that CFSR/CFSv2 presents

278   more cyclones than ERA5. The differences between datasets for the South Atlantic vary from

279   6.3% to 2.3%. The largest difference occurs in JJA, the most active cyclonic season. By choosing

280   ERA5 as the reference, the CFSv2 improves the cyclone representation in the South Atlantic

281   when compared to its antecessor, since there is a reduction of differences between CFSv2 and

282   ERA5 when compared to CFSR and ERA5. It is not possible to conclude the same for the North

283   Atlantic, which presents a small increase or decrease of differences depending on the season.

284   The spatial distribution and intensity differences between ERA5 and CFSR/CFSv2 are

285   presented in the following subsections. The results focus on the storm track active season in each

286   ocean basin: boreal winter (DJF) for the North Atlantic, and austral winter (JJA) for the South

287   Atlantic.

288

289   *3.2.1.   Spatial distribution*

290   The winter genesis and track density differences between the two datasets are presented in

291   Figure 6 for the North Atlantic (DJF) and South Atlantic (JJA). The difference is computed as

292   CFSR/CFSv2 minus ERA5, so positive (negative) values indicate that the CFSR/CFSv2 has

293   more (less) genesis or tracks in a location. Areas with significant differences (p-value < 0.01) are

294   marked with a black dot. First, for the North Atlantic, the track density difference shows that

295   ERA5 have more storm tracks than CFSR/CFSv2. The track differences do not show any dipole

13

296 patterns that would indicate shifts between storm tracks but, instead, the negative values are

297 distributed all over the main North Atlantic storm track paths from the eastern portion of the

298 eastern USA to Iceland and the UK. However, there are some local differences in genesis density

299 comparisons. The CFSR/CFSv2 presents a more concentrated genesis along the eastern coast of

300 North American, between 40ºN and 55ºN, and offshore areas. This genesis difference along the

301 coast generates an eastward shift of the east of North Atlantic genesis region between the two

302 datasets. The CFSR/CFSv2 also presents an active genesis region closer to the UK (15ºW) than

303 ERA5 (25ºW). Differences are larger in the South Atlantic, both in genesis and track densities.

304 The track density differences show that ERA5 presents a higher track density in most of the

305 domain, particularly where the South Atlantic storm track is typically found, between 40ºS and

306 55ºS, following the spiral pattern typical of the winter. Moreover, in the southwest of the domain,

307 in the Drake Passage (55ºS and 66ºS), there is a pronounced difference associated with cyclones

308 that come from the South Pacific Ocean. The genesis density difference shows that the

309 cyclogenesis regions over Uruguay and Argentina are more active in ERA5, while CFSR/CFSv2

310 favors genesis in the oceanic portion off of South America Eastern coast and Southeast of South

311 Atlantic. The genesis region in the Antarctic Peninsula is more active in ERA5, which are

312 connected to more cyclonic perturbations coming from the South Pacific.

313

314 *3.2.2. Cyclone intensity and additional characteristics*

315 Some important cyclones characteristics are shown in Table 2 for ERA5, CFSR/CFSv2,

316 CFSv2 and CFSR, for both oceanic basins. First, the mean initial vorticity is calculated by the

317 filtered vorticity (T42) at the time of the genesis in each track. The CFSR/CFSv2 presents larger

318 initial vorticity than ERA5, in all periods considered. The difference is larger for the South

319 Atlantic, where CFSR/CFSv2 cyclones are 10.4% more intense at the time of the genesis than

320 cyclones in ERA5. For the North Atlantic cyclones, CFSR/CFSv2 present storms 6.4% more

321 intense than ERA5. The cyclone propagation speed is similar between datasets, which is

322 expected once it is mainly dictated by the large scale flow. As is possible to see, regarding

323 cyclones' mean characteristics, the differences between ERA5 and CFSR/CFSv2 are small, and

324 not significant due to the large variance. Analyzing CFSR and CFSv2 separately, the differences

325 compared to ERA5 decrease in version 2. Despite the large standard deviation, the mean values

326 indicate that ERA5 cyclones seem to live longer and move further than CFSR/CFSv2 ones. To

327 investigate further the duration and displacement differences between the two datasets the

328 histograms of those cyclones characteristics are presented in Figure 7. In fact, the lifetime and

329 displacement distributions show that CFSR/CFSv2 presents a larger portion of small-distance

330 and short-life cyclones when compared to ERA5.

331   The intensity distributions are shown in Figure 8 for both the North Atlantic (DJF) and South

332 Atlantic (JJA) in two periods: from 1979 to 2019, and April/2011 to 2019, the last referring to

333 CFSv2 solely. Figure 8 also shows the intensity distribution of the matched tracks between

334 datasets. The percentage of matched tracks between ERA5 and CFSR/CFSv2 can be found in

335 Table 3. The maximum 10-m wind speed distribution for all cyclones shows that the

336 CFSR/CFSv2 presents more intense cyclones than ERA5, as its distribution is shifted to the

337 right. The mean maximum surface winds and percentiles of the distributions are displayed in

338 Table 4. CFSR/CFSv2 presents a higher mean and percentiles, and the differences between the

339 datasets are larger for the South Atlantic than North Atlantic. Additionally, the CFSv2 has a

340 broader distribution when compared to ERA5, although this is more evident in the North

341 Atlantic. The same behavior was observed by Hodges et al. (2011) when they compared CFSR

342   and ERA-Interim. The tendency of CFSR/CFSv2 to simulate more intense storms is reported by

343   previous studies (Hodges et al., 2011; Stopa and Cheung, 2014; Gramcianinov et al., 2020b). The

344   matching storms distribution reveals more about the dissimilarities between the datasets since it

345   compares the same storm simulated in each one. The intensity distribution of the matched tracks

346   is very similar to the distribution obtained with all tracks, due to the high correspondence

347   percentage between datasets (Table 3). Even for the matching cyclones distributions,

348   CFSR/CFSv2 cyclones are more intense than ERA5 ones, reinforcing its tendency to simulate

349   stronger storms. Analysing CFSR alone (not shown) does not change this behavior, but the

350   intensity distributions computed for CFSv2 and ERA5 between April/2011 and 2019, present a

351   slight increase in cyclones intensity in relation to the mean and past distribution. The distribution

352   computed for the end of the period is shifted to the right, and has a more pronounced tail to the

353   right side of maximum wind speed axis.

354

4. Discussion

356   The cyclone climatologies covering 41-years produced from ERA5 and CFSR/CFSv2 are in

357   good agreement with past studies for the North Atlantic (e.g., Hoskins and Hodges, 2002; Trigo,

358   2006; Dacre and Gray, 2009) and South Atlantic Oceans (e.g., Hoskins and Hodges, 2005;

359   Gramcianinov et al., 2019). Differences in genesis and track densities between the present and

360   past studies are expected, particularly due to the use of distinct cyclone tracking methods,

361   domains, and thresholds that define whether a cyclonic feature is a cyclone or not (Pinto et al.,

362   2005). The climatologies presented in this work show a higher cyclone density than Hoskins and

363   Hodges (2002, 2005), Dacre and Gray (2009), and Grise et al. (2013), since these authors remove

364   from their climatology cyclones that live less than 48h, which represent a large portion of the

365 systems in this study (Figure 7). However, when compared to Trigo (2006) and Gramcianinov et

366 al (2019), which also used the 24 hours as cyclone lifetime threshold, the densities presented in

367 this work are comparable (Figures 2-5). Genesis density in regions such as Greenland, in the

368 North Atlantic, and the southeastern Brazilian coast, in the South Atlantic, seem to be enhanced

369 by the addition of short-lived cyclones included in the statistics. These regions are also

370 highlighted when a smaller displacement threshold is applied (Figure 1). Crespo et al. (2020b)

371 showed five genesis region in South America without the application of any displacement

372 threshold, contrasting the three well-known cyclogenetic regions (Hoskins and Hodges, 2005;

373 Reboita et al., 2010; Gramcianinov et al., 2019). The use of displacement threshold is necessary

374 to avoid the inclusion of thermal and continental lows in the climatology, which may not develop

375 into a cyclone.

376   Another source of discrepancies between the present and previous studies is the use of 1-

377 hourly tracking, since most climatologies are constructed based on 6-hourly atmospheric fields.

378 The improved time-resolution tracking can result in slight differences in genesis position, such as

379 can be observed on the East South American coast. Despite the same tracking method and

380 thresholds, this work present a higher genesis density in Uruguay and a smaller density in the

381 Southeast Brazilian coast than Gramcianinov et al. (2019), which can be associated with the

382 identification of cyclones at earlier lifecycle stages with the use of 1-hourly tracking, instead of

383 6-hourly. Gramcianinov et al. (2019) used an artificial orographic barrier to impose an Andes

384 constraint to their tracking method, which could influence the genesis region position in their

385 work.

386   Regarding the main differences between the two data sets, ERA5 presents 3.7% more

387 cyclones than CFSR/CFSv2 (45.2 cyclones per year), which can be related to the higher

388   resolution of the former. The higher amount of cyclones in the ERA5 impacts the spatial

389   distribution differences both in the North Atlantic and South Atlantic. The track density

390   difference shows a homogeneous distribution in the major part of both domains and does not

391   reveal a shift between the tracks of the two datasets. The direct relation between model

392   resolution and the number of detected cyclones are indicated in many studies (e.g., Bengtsson et

393   al., 2006). The impact of resolution is affected by the orography representation and small-scale

394   processes important to genesis and growth. Therefore, the T42 filtering before the identification

395   process and tracking does not completely exclude the effects of the resolution on the

396   representation of cyclones in ERA5.

397   Cyclogenesis density differences show that CFSR/CFSv2 favors genesis off coast and above

398   the ocean sector, which induce a bias in genesis region along East of the North American coast

399   and Southwest of South American coast when compared to ERA5. This meridional shift in

400   genesis regions may also be related to resolution, once the best representation of orography, land

401   contrast and sea surface temperature can lead to early cyclone detection (e.g., Bengtsson et al.,

402   2006) in the ERA5. However, the differences in genesis densities are evidence of differences in

403   the track lengths between the two datasets. ERA5 presents cyclones that lived longer and travel

404   further than CFSR/CFSv2 (Figure 7), which can be addressed to the inconsistency between

405   forecast and analysis sequential time-steps. Abrupt changes in atmospheric patterns between the

406   forecast and analysis time-step can interrupt a track, breaking a unique cyclone track into two.

407   This continuity issue in CFSR/CFSv2 influences its genesis density, and also its stronger initial

408   vorticity, since a broken track leads to a new track that starts in a more mature stage of the

409   cyclone.

410   Cyclone annual mean and mean characteristics, such as displacement speed and initial

411   vorticity are similar between the two datasets, and their differences are less than 1 standard

412   deviation. Moreover, the track correspondence between the two datasets is high, being higher

413   than 90% to the whole period. In Hodges et al. (2011), the differences between more recent

414   datasets, ERA-Interim and CFSR, were smaller when compared to other older and coarser

415   resolution reanalysis. Both ERA5 and CFSR/CFSv2 are considered to be high-resolution global

416   products, and state of the art for analysis and reanalysis methodology.

417   The most pronounced difference is in the intensity distribution, which shows more intense

418   cyclones in CFSR/CFSv2 than in ERA5. The CFS family present a tendency to represent more

419   intense cyclones, winds and, consequently waves, as reported by several works (e.g., Hodges et

420   al., 2011; Stopa and Cheung, 2014; Gramcianinov et al., 2020b). There are no significant

421   difference between ERA5 and CFSR/CFSv2 when mean maximum wind speed is considered,

422   but the differences increase in the higher percentiles of the distributions (Table 4). The 10-m

423   wind components are diagnostic variables, and their computation depends on the different

424   boundary layers models component of each dataset. Even so, these parameters are widely used in

425   oceanography and ocean engineering studies and the evaluation of cyclone intensity by these

426   fields is of great value.

427   This study shows that the differences between ERA5 and CFSR/CFSv2 are larger for the

428   South Atlantic than North Atlantic. Other comparison studies found the same behavior (e.g.,

429   Hodges et al., 2003; 2011; Stoppa and Cheung, 2004). However, there is a decrease of

430   discrepancies between ERA5 and the more recent CFSv2 when compared to CFSR, particularly

431   in the South Atlantic Ocean. The decrease in differences between datasets in recent years reflects

432 the improvement of the models and increase in data availability as discussed by Hodges et al.

433 (2010).

434 The storm tracks for ERA5 and CFSR/CFSv2 used to produce the climatologies presented in

435 this work are available in ftp://masterftp.iag.usp.br/EXWAV. The provided product consists of

436 the set of monthly tracks files that contain the positional information of cyclones.

437

5. Conclusions

439 This study has evaluated and compared the cyclone climatologies for ERA5 and

440 CFSR/CFSv2 at middle and high latitudes. First, the performance of 1-hourly ERA5 and

441 CFSR/CFSv2 tracking in reproducing the Atlantic storm tracks was analyzed regarding the past

442 literature. Then, the two climatologies were compared to access the main differences between

443 them regarding the basics of storm track characteristics.

444 The storm tracks are in good agreement with past studies, both to North Atlantic (e.g.,

445 Hoskins and Hodges, 2002; Trigo, 2006; Dacre and Gray, 2009; Grise et al., 2013), and South

446 Atlantic Oceans (e.g., Gan and Rao, 1991; Mendes et al., 2010; Reboita et al., 2010;

447 Gramcianinov et al., 2019; Crespo et al., 2020b). The main North Atlantic and South Atlantic

448 storm track characteristics, such as the spiral pattern poleward, seasonal variability, and

449 latitudinal range are represented, as well as the well-known genesis regions within these ocean

450 basins. The use of hourly fields brought benefits to the tracking, particularly in areas with

451 complex terrains, such as the lee of Andes Cordillera in the South America, and East of

452 Greenland in the North Atlantic.

453 Differences between datasets showed that ERA5 has 3.7% more cyclones than CFSR/CFSv2,

454 which can be related to the finer resolution (e.g., Bengtsson et al., 2006). However, cyclone

annual mean and mean characteristics (e.g., displacement speed) are similar between the two datasets, and 90% of the tracks correspond between them. An important difference between ERA5 and CFSR/CFSv2 are the shifts in genesis density along the eastern coast, both in North and South America, which can be an indication of resolution impact in cyclone development in regions with complex orography, and temperature gradient. Furthermore, continuity issues in CFSR/CFSv2 due to jumps that might occur where forecast time-steps change to analysis time-steps can lead to broken tracks, and thus, differences between the two datasets, particularly related to genesis statistics and cyclone duration lifecycle.

Other relevant differences between ERA5 and CFSR/CFSv2 are the intensity distributions, particularly in the higher percentile of maximum 10-m wind speed. The CFSR/CFSv2 dataset presents more intense cyclones than ERA5 and this behavior persists even when CFSR and CFSv2 were evaluated separately. Other studies have already reported the ability of CFSR (Hodges et al., 2011; Stopa and Cheung, 2014) and CFSv2 (e.g., Gramcianinov et al., 2020b) to represent more extreme wind speed values. It is remarkable that in most of the analyses performed in this work, the differences between datasets decrease when CFSv2 period is analyzed separately, revealing rather a bias correction in the operational version of CFS or an increase of available data and improvement of data assimilation method. In fact, the discrepancies reduction is more pronounced in the South Atlantic, which reinforces the role of data assimilation process in the convergence of the two datasets (e.g., Hodges et al., 2011; Stopa and Cheung, 2014).

Acknowledgments

21

487

488   **References**

489   Bakhtyar, R., Orton, P.M., Marsooli, R., Miller, J.K., 2018. Rapid wave modeling of severe

490   historical extratropical cyclones off the Northeastern United States. Ocean Eng. 159, 315–

491   332. https://doi.org/10.1016/j.oceaneng.2018.04.037

492   Belmonte Rivas, M., Stoffelen, A., 2019. Characterizing ERA-Interim and ERA5 surface wind

493   biases using ASCAT. Ocean Sci. 15, 831–852. https://doi.org/10.5194/os-15-831-2019

494   Bengtsson, L., Hodges, K.I., Keenlyside, N., 2009. Will extratropical storms intensify in a

495   warmer climate? J. Clim. 22, 2276–2301. https://doi.org/10.1175/2008JCLI2678.1

496   Bengtsson, L., Hodges, K.I., Roeckner, E., 2006. Storm tracks and climate change. J. Clim. 19,

497   3518–3543. https://doi.org/10.1175/JCLI3815.1

498 Booth, J.F., Rieder, H.E., Kushnir, Y., 2016. Comparing hurricane and extratropical storm surge

499   for the Mid-Atlantic and Northeast Coast of the United States for 1979-2013. Environ. Res.

500   Lett. 11(9). 10.1088/1748-9326/11/9/094004

501 Campos, R.M., Guedes Soares, C., 2016. Comparison and Assessment of Three Wave Hindcasts

502   in the North Atlantic Ocean. J. Oper. Oceanogr. 9(1):26-44.

503   https://doi.org/10.1080/1755876X.2016.1200249

504 Campos, R.M., Guedes Soares, C., 2017. Assessment of Three Wind Reanalysis in the North

505   Atlantic Ocean. J. Oper. Oceanogr. 10(1):30-44.

506   https://doi.org/10.1080/1755876X.2016.1253328

507 Campos, R.M., Alves, J.H.G.M., Guedes Soares, C., Guimaraes, L.G., Parente, C.E., 2018.

508   Extreme wind-wave modeling and analysis in the South Atlantic Ocean. Ocean Model. 124,

509   75–93. https://doi.org/10.1016/j.ocemod.2018.02.002

510 Campos, R.M., Guedes Soares, C., Alves, J.H.G.M., Parente, C.E., Guimaraes, L.G., 2019.

511   Regional long-term extreme wave analysis using hindcast data from the South Atlantic

512   Ocean. Ocean Eng. 179, 202–212. https://doi.org/10.1016/j.oceaneng.2019.03.023

513 Chelton, D. B., Schlax, M. G., Freilich, M. H., Milliff, R. F., 2004. Satellite measurements reveal

514   persistent small-scale features in ocean winds. Science 303, 978–983,

515   https://doi.org/10.1126/science.1091901

516 Colle, B.A., Rojowsky, K., Buonaito, F., 2010. New York city storm surges: Climatology and an

517   analysis of the wind and cyclone evolution. J. Appl. Meteorol. Climatol. 49(1): 85–100.

518   10.1175/2009JAMC2189.1

519   Copernicus Climate Change Service (C3S) 2017. ERA5: Fifth generation of ECMWF

520   atmospheric reanalyses of the global climate. Copernicus Climate Change Service Climate

521   Data Store (CDS), July, 2019.

522   Crespo, N.M.; da Rocha, R.P.; De Jesus, E.M., 2020a. Cyclones density and characteristics in

523   different reanalyses dataset over South America. In: EGU General Assembly 2020, Online, 4-

524   8 May 2020, EGU2020-11316. https://doi.org/10.5194/egusphere-egu2020-11316

525   Crespo, N.M., da Rocha, R.P., Sprenger, M., Wernli, H., 2020b. A Potential Vorticity

526   Perspective on Cyclogenesis over Center-Eastern South America. Int. J. Climatol. 1-16.

527   https://doi.org/10.1002/joc.6644

528   Dacre, H.F., Gray, S.L., 2009. The spatial distribution and evolution characteristics of North

529   Atlantic   cyclones.   Mon.   Weather   Rev.   137,   99–115.

530   https://doi.org/10.1175/2008MWR2491.1

531   Dacre, H.F., Hawcroft, M.K., Stringer, M.A., Hodges, K.I., 2012. An extratropical cyclone atlas

532   a tool for illustrating cyclone structure and evolution characteristics. Bull. Am. Meteorol. Soc.

533   93, 1497–1502. https://doi.org/10.1175/BAMS-D-11-00164.1

534   Evans, J. L., Braun, A., 2012. A Climatology of Subtropical Cyclones in the South Atlantic. J.

535   Climate 25, 7328–7340, https://doi.org/10.1175/JCLI-D-11-00212.1.

536   Gan, M.A., Rao, V.B., 1991. Surface Cyclogenesis over South America. Mon. Weather Rev.

537   119, 1293–1302. https://doi.org/10.1175/1520-0493(1991)119<1293:SCOSA>2.0.CO;2

538   Gozzo, L.F., da Rocha, R.P., Reboita, M.S., Sugahara, S., 2014. Subtropical cyclones over the

539   southwestern South Atlantic: Climatological aspects and case study. J. Clim. 27, 8543–8562.

540   https://doi.org/10.1175/JCLI-D-14-00149.1

541 Gramcianinov, C.B., Campos, R.M., Guedes Soares, C., Camargo, R., 2020a. Extreme waves

542   generated by cyclonic winds in the western portion of the South Atlantic Ocean. Ocean Eng.

543   213: 107745. https://doi.org/10.1016/j.oceaneng.2020.107745

544 Gramcianinov, Campos, R.M., Guedes Soares, C., Camargo, R., 2020b. Comparison between

545   ERA5 and CFS datasets of extratropical cyclones associated with extreme wave events in the

546   Atlantic Ocean. Proceedings of the ASME 2020 29th International Conference on Offshore

547   Mechanics and Arctic Engineering, Online, 3-7 August, 2020, ASME.

548 Gramcianinov, C.B., Hodges, K.I., Camargo, R., 2019. The properties and genesis environments

549   of South Atlantic cyclones. Clim. Dyn. 53, 4115–4140. https://doi.org/10.1007/s00382-019-

550   04778-1

551 Grise, K.M., Son, S.W., Gyakum, J.R., 2013. Intraseasonal and interannual variability in north

552   american storm tracks and its relationship to equatorial pacific variability. Mon. Weather Rev.

553   141, 3610–3625. https://doi.org/10.1175/MWR-D-12-00322.1

554 Guishard, M.P., Evans, J.L., Hart, R.E., 2009. Atlantic subtropical storms. Part II: Climatology.

555   J. Clim. 22, 3574 – 3594. https://doi.org/10.1175/2008JCLI2346.1

556 Hersbach, H., Dee, D., 2016. ERA5 reanalysis is in production, ECMWF Newsletter 147,

557   ECMWF, Reading, UK, 2016.

558 Hersbach, H., Bell, B., Berrisford, P., Horányi, A., Sabater, J.M., Nicolas, J., Radu, R., Schepers,

559   D., Simmons, A., Soci, C., Dee, D., 2018. Global reanalysis: goodbye ERA-Interim, hello

560   ERA5. ECMWF Newsl. 17–24. https://doi.org/10.21957/vf291hehd7

561 Hodges, K.I., 1994. A General Method for Tracking Analysis and Its Application to

562   Meteorological Data. Mon. Weather Rev. 122, 2573–2586. https://doi.org/10.1175/1520-

563   0493(1994)122<2573:AGMFTA>2.0.CO;2

564 Hodges, K.I., 1995. Feature Tracking on the Unit Sphere. Mon. Weather Rev. 123, 3458–3465.

565 https://doi.org/10.1175/1520-0493(1995)123<3458:FTOTUS>2.0.CO;2

566 Hodges, K.I., 1996. Spherical Nonparametric Estimators Applied to the UGAMP Model

567 Integration for AMIP. Mon. Weather Rev. 124, 2914–2932. https://doi.org/10.1175/1520-

568 0493(1996)124<2914:SNEATT>2.0.CO;2

569 Hodges, K.I., 1999. Adaptive constraints for feature tracking. Mon. Weather. Rev., 127, 1362–

570 1373. https://doi.org/10.1175/1520-0493(1999)127<1362:ACFFT>2.0.CO;2

571 Hodges, K.I., 2008: Confidence intervals and significance tests for spherical data derived from

572 feature tracking. Mon. Weather Rev., 136, 1758–1777.

573 https://doi.org/10.1175/2007MWR2299.1

574 Hodges, K.I., Hoskins, B.J., Boyle, J., Thorncroft, C., 2003. A Comparison of Recent Reanalysis

575 Datasets Using Objective Feature Tracking: Storm Tracks and Tropical Easterly Waves. Mon.

576 Weather Rev. 131, 2012–2037. https://doi.org/10.1175/1520-

577 0493(2003)131<2012:ACORRD>2.0.CO;2

578 Hodges, K.I., Lee, R.W., Bengtsson, L., 2011. A comparison of extratropical cyclones in recent

579 reanalyses ERA-Interim, NASA MERRA, NCEP CFSR, and JRA-25. J Clim 24:4888–4906.

580 https://doi.org/10.1175/2011JCLI4097.1

581 Hoskins, B.J., Hodges, K.I., 2002. New Perspectives on the Northern Hemisphere Winter Storm

582 Tracks. J. Atmos. Sci. 59, 1041–1061. https://doi.org/10.1175/1520-

583 0469(2002)059<1041:NPOTNH>2.0.CO;2

584 Hoskins, B.J., Hodges, K.I., 2005. A New Perspective on Southern Hemisphere Storm Tracks. J.

585 Clim. 18, 4108–4129. https://doi.org/10.1175/JCLI3570.1

586 Jones, D.A., Simmonds, I., 1993. A climatology of Southern Hemisphere extratropical cyclones.

587   Climate Dyn. 9, 131–145. https://doi.org/10.1007/BF00209750

588 Kalnay, E., Kanamitsu, M., Kistler, R., Collins, W., Deaven, D., Gandin, L., Iredell, M., Saha,

589   S., White, G., Woollen, J., Zhu, Y., Chelliah, M., Ebisuzaki, W., Higgins, W., Janowiak, J.,

590   Mo, K.C., Ropelewski, C., Wang, J., Leetmaa, A., Reynolds, R., Jenne, R., Joseph, D., 1996.

591   The NCEP/NCAR 40-Year Reanalysis Project. Bull. Amer. Meteor. Soc., 77, 437–472.

592   https://doi.org/10.1175/1520-0477(1996)077<0437:TNYRP>2.0.CO;2

593 Kumar, V.S., Mandal, S., Kumar, K.A., 2003. Estimation of wind speed and wave height during

594   cyclones. Ocean Eng. 30, 2239–2253. https://doi.org/10.1016/S0029-8018(03)00076-3

595 Mattioli, M., De Masi, G., Drago, M., 2019. Evaluating extreme cyclonic sea states. Ocean Eng.

596   194, 106639. https://doi.org/10.1016/j.oceaneng.2019.106639

597 Mendes, D., Souza, E.P., Marengo, J.A., Mendes, M.C.D., 2010. Climatology of extratropical

598   cyclones over the South American-southern oceans sector. Theor. Appl. Climatol. 100, 239–

599   250. https://doi.org/10.1007/s00704-009-0161-6

600 Murray, R.J., Simmonds, I., 1991a. A numerical scheme for tracking cyclone centres from digital

601   data Part I: development and operation of the scheme. Aust. Meteorol. Mag. 39, 155–166.

602 Murray, R.J., Simmonds, I., 1991b. A numerical scheme for tracking cyclone centres from

603   digital data. Part II: application to January and July general circulation model simulations.

604   Aust. Meteorol. Mag. 39, 155–166.

605 Olauson, J., 2018. ERA5: The new champion of wind power modelling? Renew. Energy 126,

606   322–331. https://doi.org/10.1016/j.renene.2018.03.056

607 Onogi, K., Tsutsui, J., Koide, H., Sakamoto, M., Kobayashi, S., Hatsushika, H., Matsumoto, T.,

608   Yamazaki, N., Kamahori, H., Takahashi, K., Kadokura, S., Wada, K., Kato, K., Oyama, R.,

609   Ose, T., Mannoji, N., Taira, R., 2007. The JRA-25 Reanalysis. J. Meteorol. Soc. Japan. Ser. II

610   85, 369–432. https://doi.org/10.2151/jmsj.85.369

611   Parker, W.S., 2016. Reanalyses and observations: What's the Difference? Bull. Am. Meteorol.

612   Soc. 97, 1565–1572. https://doi.org/10.1175/BAMS-D-14-00226.1

613   Pinto, J.G., Spangehl, T., Ulbrich, U., Speth, P., 2005. Sensitivities of a cyclone detection and

614   tracking algorithm: Individual tracks and climatology. Meteorol. Zeitschrift 14, 823–838.

615   https://doi.org/10.1127/0941-2948/2005/0068

616   Ponce De León, S., Guedes Soares, C., 2012. Distribution of winter wave spectral peaks in the

617   seas around Norway. Ocean Eng. 50, 63–71. https://doi.org/10.1016/j.oceaneng.2012.05.005

618   Raible, C.C., Della-Marta, P.M., Schwierz, C., Wernli, H., Blender, R., 2008. Northern

619   Hemisphere Extratropical Cyclones: A Comparison of Detection and Tracking Methods and

620   Different   Reanalyses.   Mon.   Weather   Rev.   136,   880–897.

621   https://doi.org/10.1175/2007MWR2143.1

622   Reboita, M.S., da Rocha, R.P., Ambrizzi, T., Sugahara, S., 2010. South Atlantic Ocean

623   cyclogenesis climatology simulated by regional climate model (RegCM3). Clim. Dyn. 35,

624   1331–1347. https://doi.org/10.1007/s00382-009-0668-7

625   Reboita, M.S., da Rocha, R.P., de Souza, M.R., Llopart, M., 2018. Extratropical cyclones over

626   the southwestern South Atlantic Ocean: HadGEM2-ES and RegCM4 projections. Int. J.

627   Climatol. 38, 2866–2879. https://doi.org/10.1002/joc.5468

628   Rienecker, M.M., Suarez, M.J., Gelaro, R., Todling, R., Bacmeister, J., Liu, E., Bosilovich,

629   M.G., Schubert, S.D., Takacs, L., Kim, G., Bloom, S., Chen, J., Collins, D., Conaty, A., da

630   Silva, A., Gu, W., Joiner, J., Koster, R.D., Lucchesi, R., Molod, A., Owens, T., Pawson, S.,

631   Pegion, P., Redder, C.R., Reichle, R., Robertson, F.R., Ruddick, A.G., Sienkiewicz, M..

632   Woollen, J., 2011. MERRA: NASA's Modern-Era Retrospective Analysis for Research and

633   Applications. J. Climate, 24, 3624–3648

634   Saha, S., Moorthi, S., Pan, H., Wu, X., Wang, J., Nadiga, S., Tripp, P., Kistler, R., Woollen, J.,

635   Behringer, D., Liu, H., Stokes, D., Grumbine, R., Gayno, G., Wang, J., Hou, Y., Chuang, H.,

636   Juang, H.H., Sela, J., Iredell, M., Treadon, R., Kleist, D., Delst, P. Van, Keyser, D., Derber,

637   J., Ek, M., Meng, J., Wei, H., Yang, R., Lord, S., Dool, H. van den, Kumar, A., Wang, W.,

638   Long, C., Chelliah, M., Xue, Y., Huang, B., Schemm, J., Ebisuzaki, W., Lin, R., Xie, P.,

639   Chen, M., Zhou, S., Higgins, W., Zou, C., Liu, Q., Chen, Y., Han, Y.,Cucurull, L., Reynolds,

640   R.W., Rutledge, G., Goldberg, M., 2010. The NCEP Climate Forecast System Reanalysis.

641   Bull. Amer. Meteor. Soc., 91, 1015–1058. https://doi.org/10.1175/2010BAMS3001.1

642   Saha, S., S. Moorthi, S., Wu, X., Wang, J., Nadiga, S., Tripp, P, Behringer, D., Hou, Y., Chuang,

643   H., Iredell, M., Ek, M., Meng, J., Yang, R., Mendez, M.P., Dool, H. van den, Zhang, Q.,

644   Wang, W., Chen, M., Becker, E., 2014. The NCEP Climate Forecast System Version 2. J.

645   Climate, 27, 2185–2208. https://doi.org/10.1175/JCLI-D-12-00823.1

646   Sebastian, M., Behera, M.R., Murty P.L.N., 2019. Storm surge hydrodynamics at a concave

647   coast   due   to   varying   approach   angles   of   cyclone.   Ocean.   Eng.   191.

648   https://doi.org/10.1016/j.oceaneng.2019.106437

649   Simmonds, I., Keay, K., 2000. Mean southern hemisphere extratropical cyclone behavior in the

650   40-year   NCEP-NCAR   reanalysis.   J.   Clim.   13,   873–885.   https://doi.org/10.1175/1520-

651   0442(2000)013<0873:MSHECB>2.0.CO;2

652   Simmonds, I., Keay, K., 2000. Mean southern hemisphere extratropical cyclone behavior in the

653   40-year   NCEP-NCAR   reanalysis.   J.   Clim.   13,   873–885.   https://doi.org/10.1175/1520-

654   0442(2000)013<0873:MSHECB>2.0.CO;2

655   Simmons, A., Uppala, S., Dee, D., Kobayashi, S., 2007. ERA-Interim: New ECMWF reanalysis

656   products from 1989 onwards. ECMWF Newsletter 110, ECMWF, Reading, UK, 25–35.

657   Sinclair, M.R., 1994. An objective cyclone climatology for the Southern Hemisphere. Mon. Wea.

658   Rev., 122, 2239–2256.

659   Sinclair, M.R., 1997. Objective Identification of Cyclones and Their Circulation Intensity, and

660   Climatology. Weather Forecast. 12, 595–612. https://doi.org/10.1175/1520-

661   0434(1997)012<0595:OIOCAT>2.0.CO;2

662   Stopa, J.E., Cheung, K.F., 2014. Intercomparison of wind and wave data from the ECMWF

663   Reanalysis Interim and the NCEP Climate Forecast System Reanalysis. Ocean Model. 75,

664   65–83.

665   Trigo, I.F., 2006. Climatology and interannual variability of storm-tracks in the Euro-Atlantic

666   sector: A comparison between ERA-40 and NCEP/NCAR reanalyses. Clim. Dyn. 26, 127–

667   143. https://doi.org/10.1007/s00382-005-0065-9

668   Vettor, R., Guedes Soares, C., 2016. Rough weather avoidance effect on the wave climate

669   experienced by oceangoing vessels. Appl. Ocean Res. 59, 606–615.

670   https://doi.org/10.1016/j.apor.2016.06.004

671   Vettor, R., Guedes Soares, C., 2017. Characterization of the expected weather conditions in the

672   main European coastal traffic routes. Ocean Eng. 140, 244–257.

673   https://doi.org/10.1016/j.oceaneng.2017.05.027

674

Tables

676 **Table 1.** Mean number of cyclones tracked in ERA5 and CFSR/CFSv2 between 1979 and 2019, annual

677 and seasonal mean. The mean are also computed for CFSR (1979-March/2011) and CFSv2 (April/2011-

678 2019) alone. All cyclones that pass within the extratropical latitudes of the South Atlantic (SA; 85ºS-25ºS,

679 75ºW-20ºE) and North Atlantic (NA; 85ºN-25ºN, 65ºW-0ºE) Oceans were considered.

| | | **1979-2019** | | | | |
		Annual	**DJF**	**MAM**	**JJA**	**SON**
NA	**ERA5**	551.0 ± 23.6	155.8 ± 9.7	140.9 ± 10.6	117.5 ± 8.3	136.7 ± 9.1
	CFSR/CFSv2	538.7 ± 21.2	152.9 ± 8.1	135.2 ± 11.3	118.0 ± 7.9	132.7 ± 8.8
SA	**ERA5**	730.9 ± 21.4	158.2 ± 10.0	184.8 ± 11.5	201.9 ± 11.7	186.0 ± 9.9
	CFSR/CFSv2	698.0 ± 19.7	154.2 ± 9.6	177.1 ± 10.6	189.3 ± 10.2	177.4 ± 10.0
		1979-2011				
		Annual	**DJF**	**MAM**	**JJA**	**SON**
NA	**ERA5**	537.8 ± 72.5	154.4 ± 14.8	137.7 ± 16.4	117.5 ± 8.7	135.8 ± 8.9
	CFSR	525.2 ± 69.9	151.7 ± 12.9	131.7 ± 16.9	117.5 ± 7.3	131.8 ± 8.4
SA	**ERA5**	709.2 ± 100.4	155.0 ± 14.1	180.9 ± 24.5	200.3 ± 11.8	184.6 ± 10.6
	CFSR	678.7 ± 97.5	151.5 ± 14.4	174.3 ± 24.3	187.8 ± 10.1	176.2 ± 10.4
		2011-2019				
		Annual	**DJF**	**MAM**	**JJA**	**SON**
NA	**ERA5**	538.1 ± 52.9	143.8 ± 36.6	137.2 ± 18.6	117.6 ± 7.0	139.6 ± 9.4
	CFSv2	528.6 ± 54.0	140.0 ± 35.6	133.1 ± 16.6	119.8 ± 10.0	135.7 ± 10.0
SA	**ERA5**	729.3 ± 57.9	152.4 ± 33.9	178.4 ± 22.3	207.7 ± 9.8	190.8 ± 5.1
	CFSv2	691.0 ± 61.2	147.1 ± 30.9	167.8 ± 21.6	194.6 ± 9.5	181.6 ± 7.6

680

681

682

683

684

685

686

687 **Table 2.** Mean characteristics of cyclones for ERA5 and CFSR/CFSv2 (1979-2019), and computed for
688 for CFSR (1979-March/2011) and CFSv2 (April/2011-2019) separately. Initial vorticity is the filtered
689 relative vorticity at the time of genesis, and is scaled by -1 in South Atlantic. Displacement is computed
690 using the first and the last track point. All cyclones that pass within the extratropical latitudes of the South
691 Atlantic (SA; 85ºS-25ºS, 75ºW-20ºE) and North Atlantic (NA; 85ºN-25ºN, 65ºW-0ºE) Oceans were
692 considered.

		1979 - 2019			
		Initial vorticity (CVU)	**Lifetime (days)**	**Displacement (m)**	**Speed (km h^{-1})**
NA	**ERA5**	2.7 ± 1.4	4.4 ± 3.0	2928.5 ± 1582.2	9.6 ± 4.7
	CFSR/CFSv2	2.8 ± 1.5	4.0 ± 2.6	2767.8 ± 1467.6	9.8 ± 4.6
SA	**ERA5**	2.9 ± 1.5	3.9 ± 2.6	3712.0 ± 2157.9	13.2 ± 5.3
	CFSR/CFSv2	3.2 ± 1.6	3.3 ± 2.1	3228.3 ± 1855.6	13.3 ± 5.3
		1979 - 2011			
		Initial vorticity (CVU)	**Lifetime (days)**	**Displacement (m)**	**Speed (km h^{-1})**
NA	**ERA5**	2.7 ± 1.4	4.4 ± 2.9	2919.2 ± 1569.4	9.6 ± 4.6
	CFSR	2.9 ± 1.5	4.0 ± 2.6	2750.6 ± 1452.6	9.8 ± 4.6
SA	**ERA5**	2.9 ± 1.5	3.9 ± 2.6	3688.0 ± 2146.9	13.2 ± 5.3
	CFSR	3.3 ± 1.6	3.2 ± 2.1	3155.5 ± 1799.8	13.3 ± 5.3
		2011 - 2019			
		Initial vorticity (CVU)	**Lifetime (days)**	**Displacement (m)**	**Speed (km h^{-1})**
NA	**ERA5**	2.7 ± 1.5	4.5 ± 3.1	2962.5 ± 1628.0	9.6 ± 4.8
	CFSv2	2.8 ± 1.6	4.1 ± 2.7	2830.7 ± 1519.6	9.8 ± 4.7
SA	**ERA5**	3.0 ± 1.5	4.0 ± 2.7	3797.7 ± 2194.7	13.3 ± 5.4
	CFSv2	3.2 ± 1.6	3.6 ± 2.3	3490.3 ± 2022.5	13.4 ± 5.3

693

694 **Table 3.** Percentage of the number of matched tracks for ERA5 and CFSR/CFSv2 (1979-2019), CFSR
695 (1979-March/2011), and CFSv2 (April/2011-2019). Similar tracks are obtained in DJF for the North
696 Atlantic (NA), and JJA for the South Atlantic (SA) Oceans.

|		**1979 - 2019**	**1979 - 2011**	**2011 - 2019**
NA	**ERA5**	92.7%	91.9%	87.1%
	CFSR/CFSv2	96.0%	94.9%	91.1%
SA	**ERA5**	93.1%	91.8%	89.2%
	CFSR/CFSv2	96.5%	95.4%	91.8%

697

Table 4. Mean maximum 10-m wind speed (m s^{-1}) and percentiles of cyclones for ERA5 and CFSR/CFSv2 (1979-2019) in DJF for the North Atlantic (NA), and JJA for the South Atlantic (SA) Oceans. Matched cyclones are identical storms find in both datasets.

		ERA5				CFSR/CFSv2			
		mean	50%	90%	95%	mean	50%	90%	95%
NA	all	21.4 ±5.1	21.1	28.2	30.1	23.9 ± 6.4	23.7	32.5	35.0
	matched	21.5 ±5.1	21.2	28.3	30.2	24.0 ± 6.4	23.8	32.6	35.0
SA	all	21.2 ± 4.8	21.0	27.3	29.3	23.4 ± 4.8	23.3	30.2	32.1
	matched	21.2 ± 4.8	21.0	27.4	29.3	23.4 ± 5.3	23.4	30.2	32.2
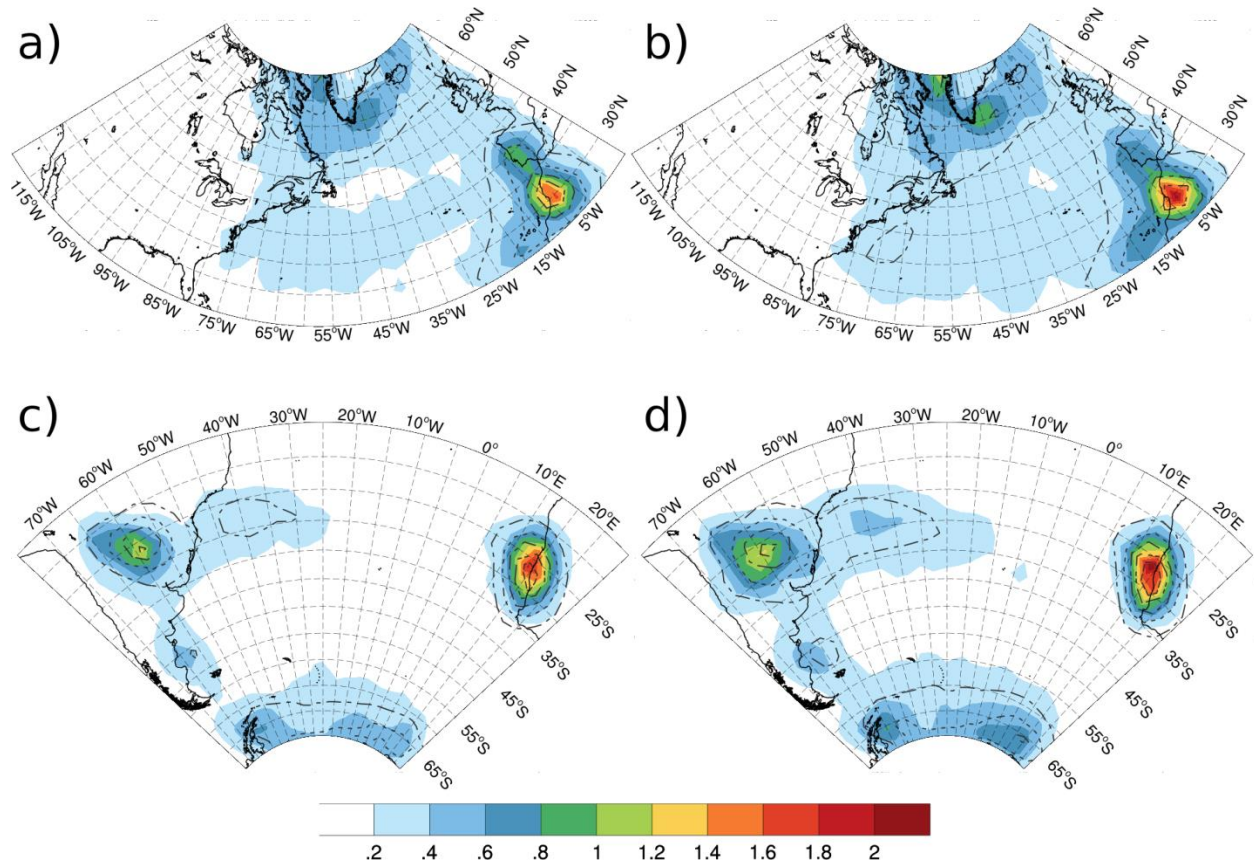
Figures

Figure 1. Genesis (shaded) and track (contour) densities computed for cyclones that last at least 24 hour and travel less than 1000 km for the (a) North Atlantic in ERA5 and (b) CFSR/CFSv2, and (c) South Atlantic in ERA5 and (d) CFSR/CFSv2. The density unit is cyclones/track per month per area, where the unit area is equivalent to a 5° spherical cap (10^6 km^2). The track density contour are with contour interval 1 track per month per area, and the densities are calculated for 1979-2019.

705

706

707

708

709

710

711

712

713

34
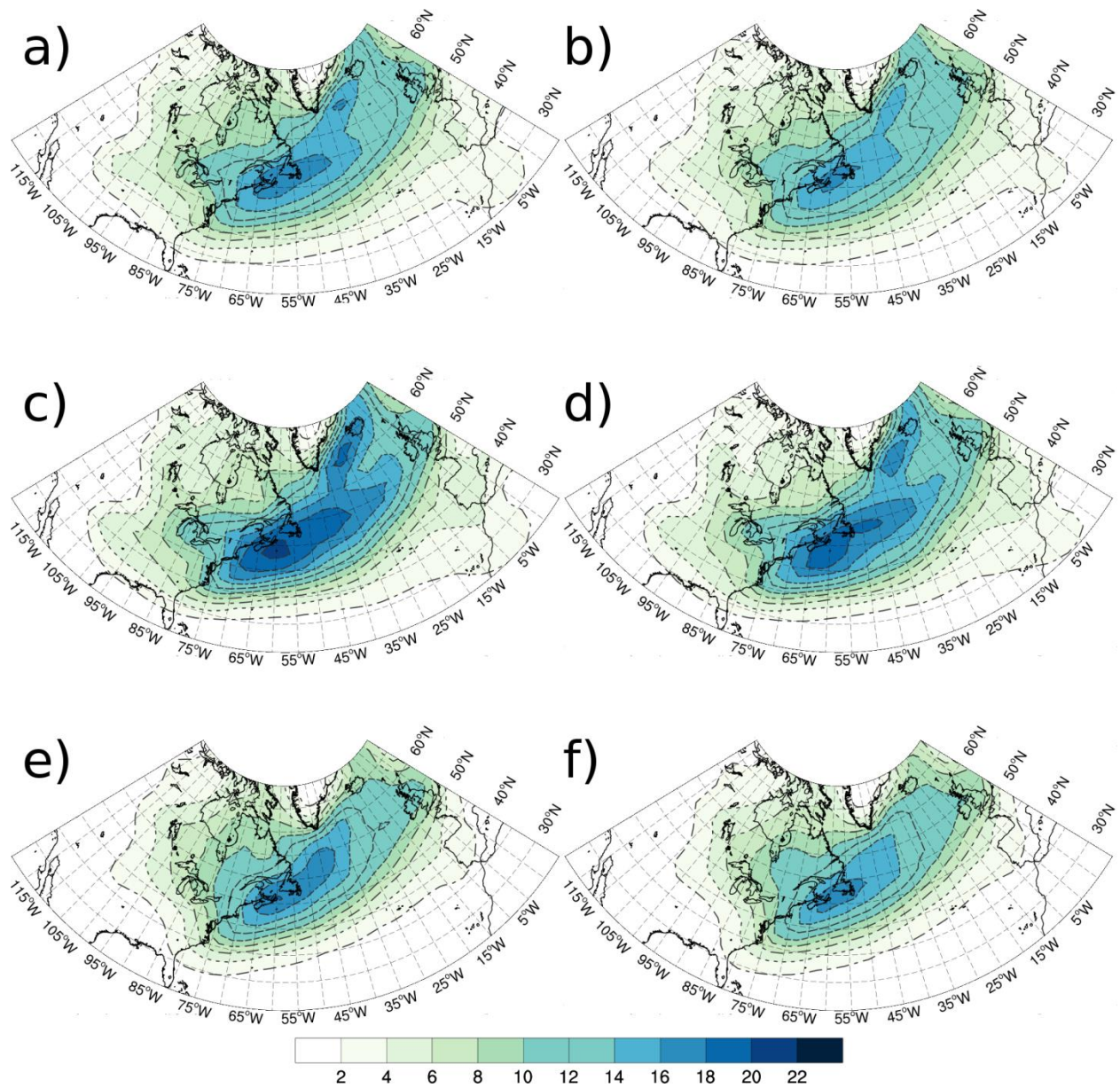
Figure 2. Track densities computed for the North Atlantic in (a,c,e) ERA5 and (b,d,f) CFSR/CFSv2, considering (a,b) all period (1979-2019), (c,d) DJF, and (e,f) JJA. The density unit is track per month per area, where the unit area is equivalent to a 5° spherical cap (10^6 km^2). The contour interval is 2 tracks per month per area.
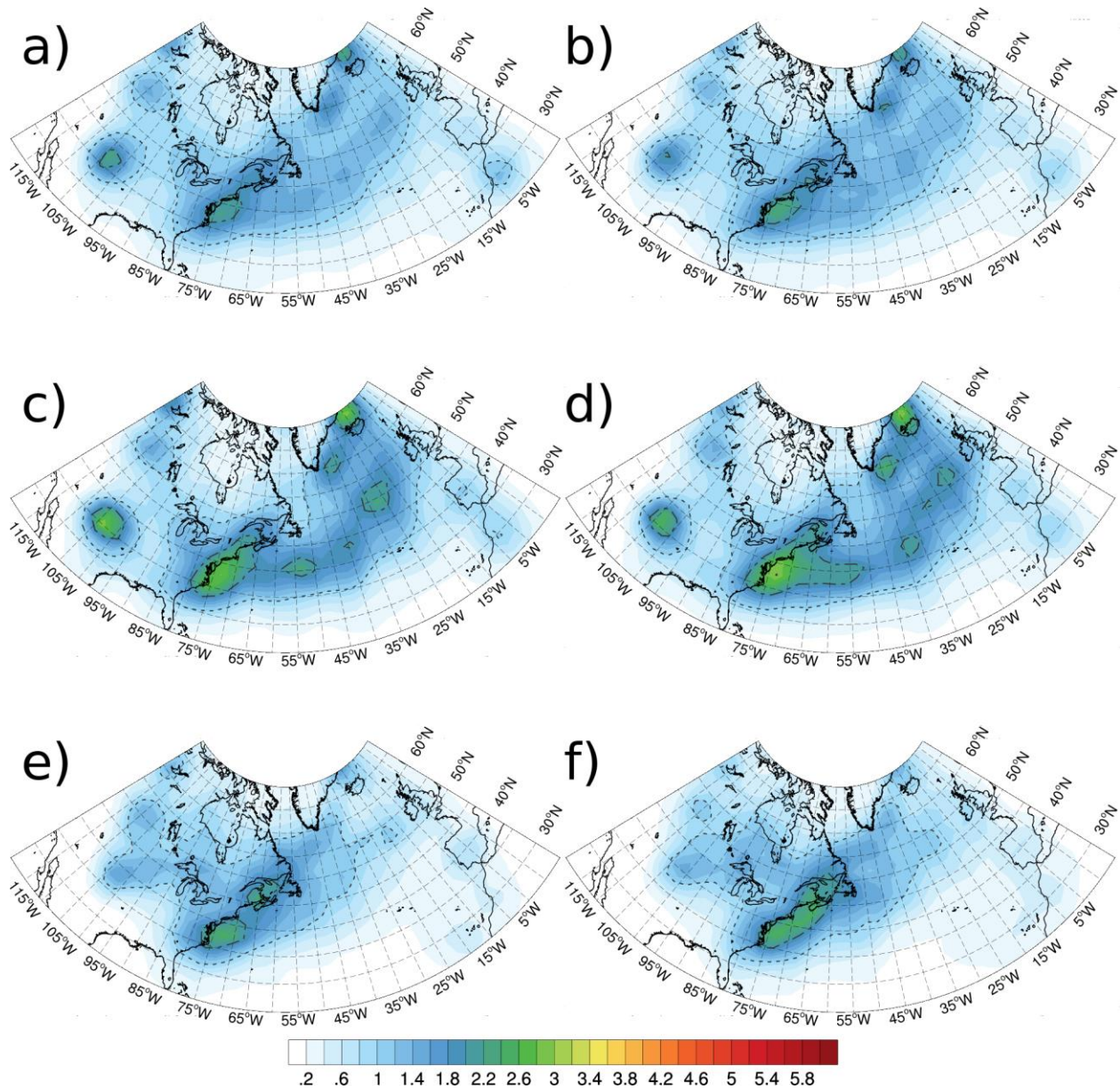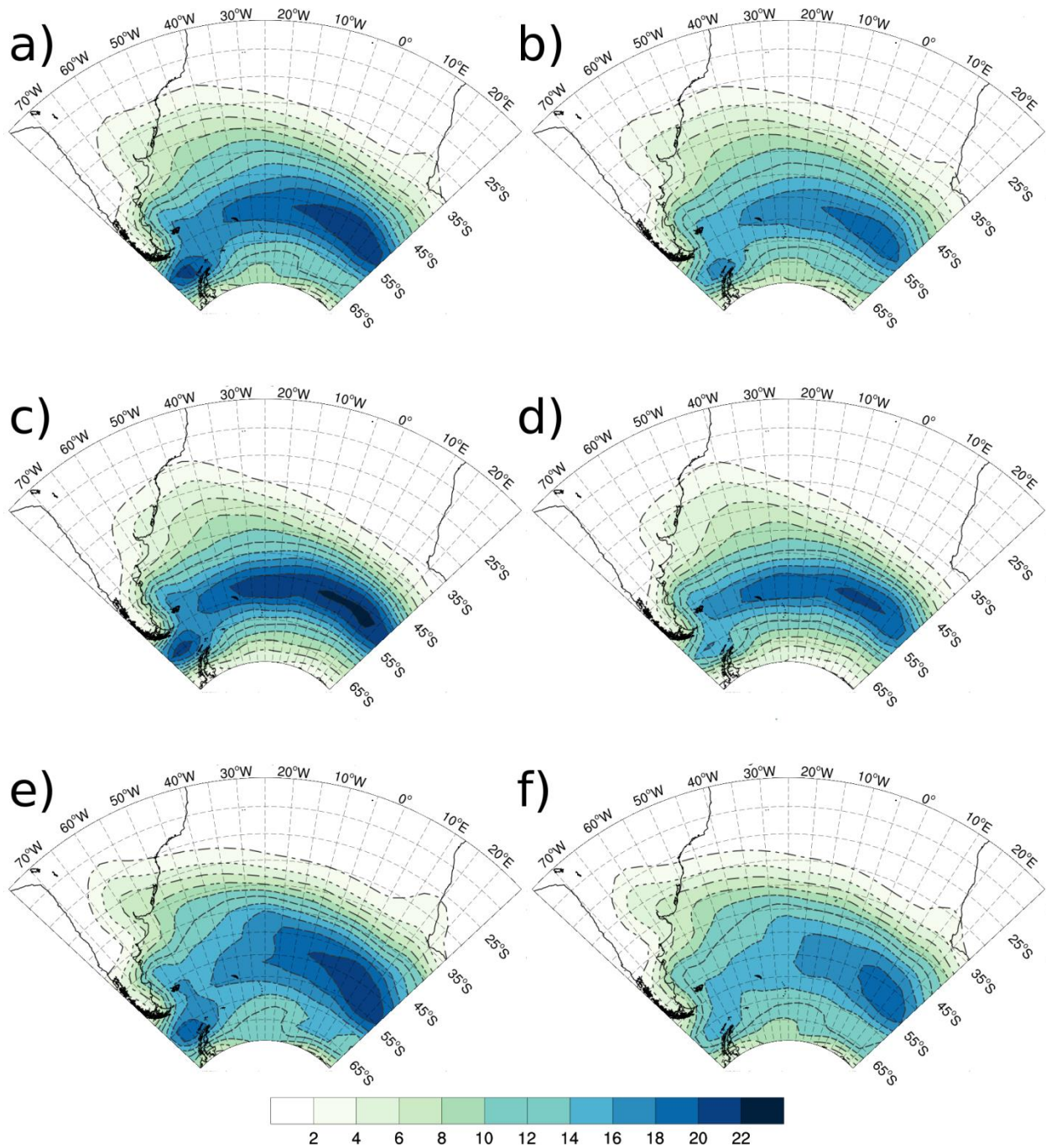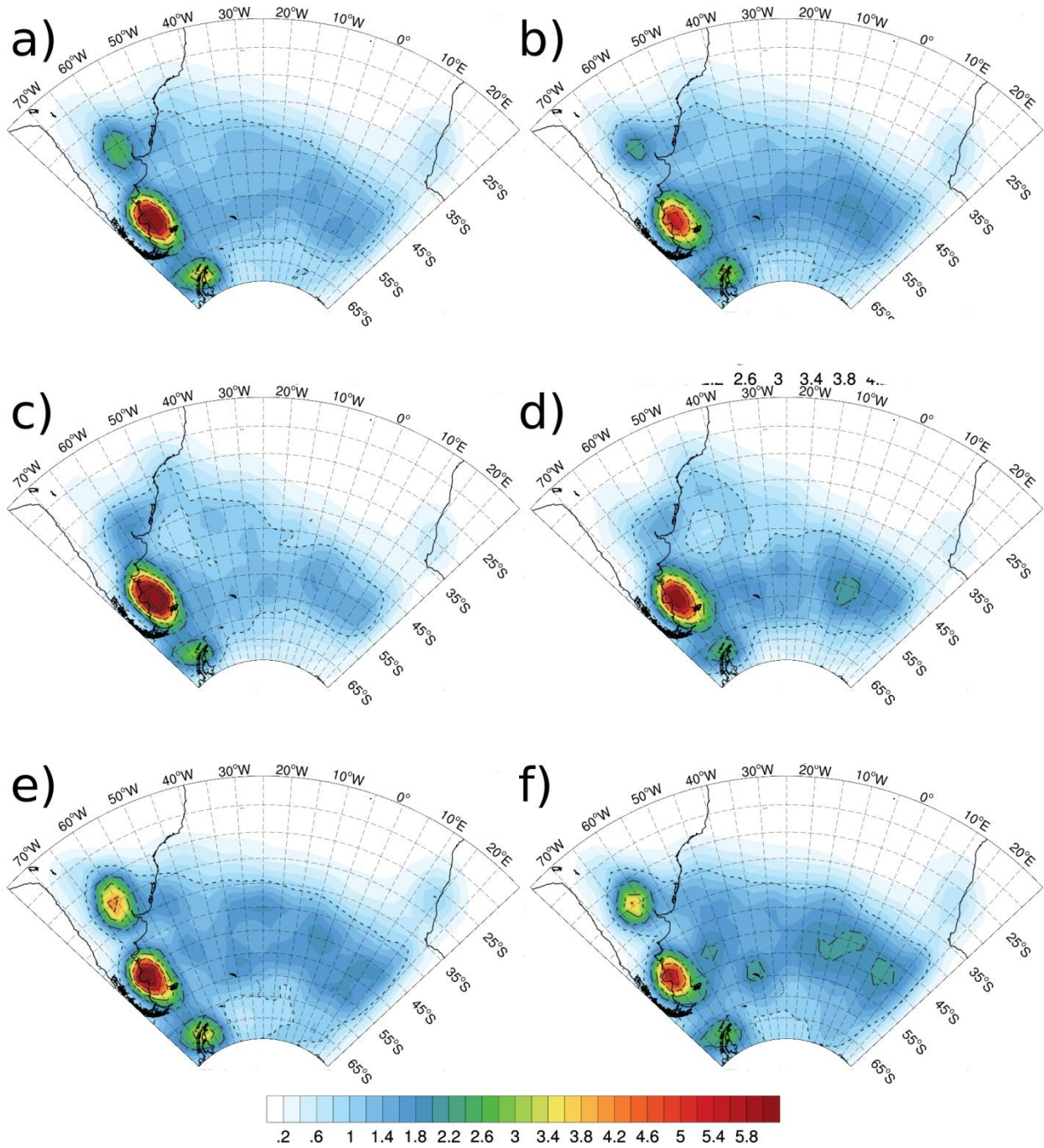
714

Figure 3. Genesis densities computed for the North Atlantic in (a,c,e) ERA5 and (b,d,f) CFSR/CFSv2, considering (a,b) all period (1979-2019), (c,d) DJF, and (e,f) JJA. The density unit is genesis per month per area, where the unit area is equivalent to a 5° spherical cap (10^6 km^2). The contour interval is 1 genesis per month per area.

715

716

717

Figure 4. Track densities computed for the South Atlantic in (a,c,e) ERA5 and (b,d,f) CFSR/CFSv2, considering (a,b) all period (1979-2019), (c,d) DJF, and (e,f) JJA. The density unit is track per month per area, where the unit area is equivalent to a 5º spherical cap (10^6 km^2). The contour interval is 2 tracks per month per area.

718

37

Figure 5. Genesis densities computed for the South Atlantic in (a,c,e) ERA5 and (b,d,f) CFSR/CFSv2, considering (a,b) all period (1979-2019), (c,d) DJF, and (e,f) JJA. The density unit is genesis per month per area, where the unit area is equivalent to a 5° spherical cap (10^6 km^2). The contour interval is 1 genesis per month per area.
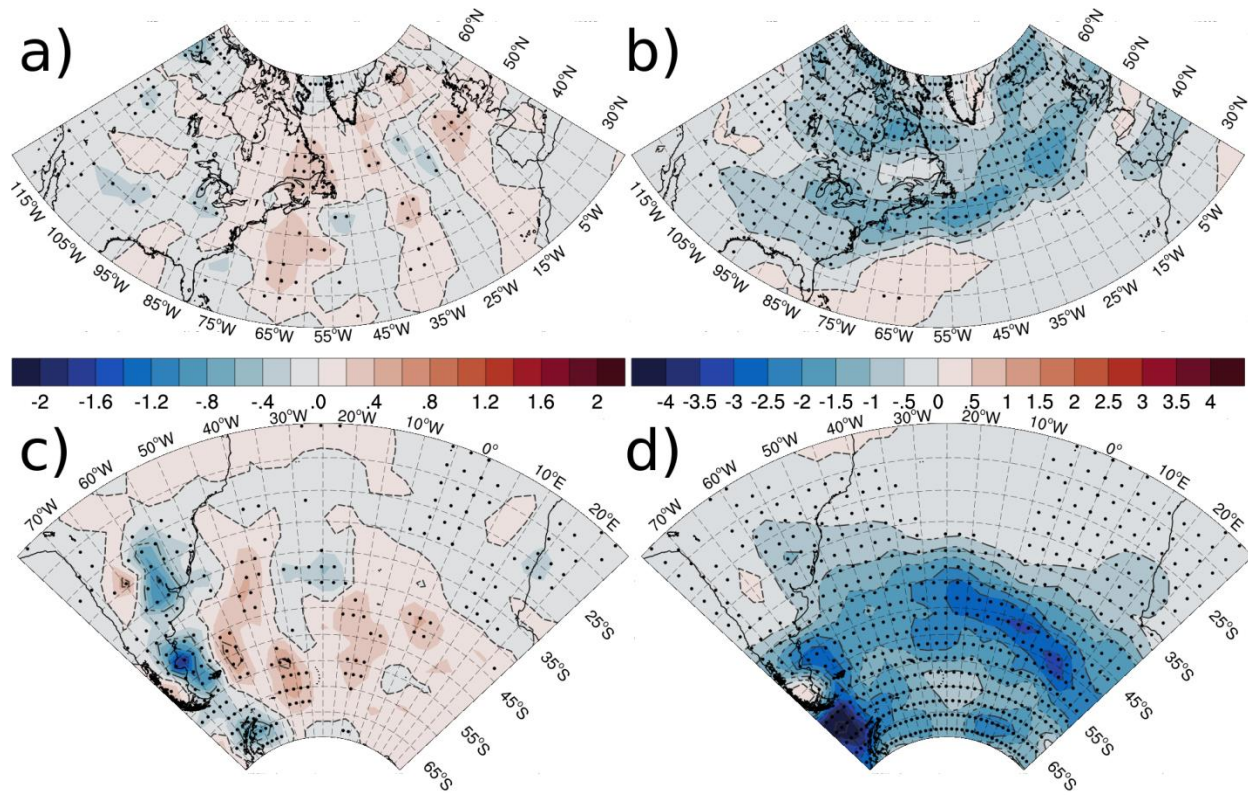
719

38

Figure 6. Densities differences in (a,b) DJF for the North Atlantic and (c,d) JJA for the South Atlantic, for the (a,c) cyclogenesis and (b,d) storm track. The density difference unit is cyclones/track per month per area, where the unit area is equivalent to a 5° spherical cap (10^6 km^2). The dots represent grid points where the trend is significant within 99% confidence level, and the differences are CFSR/CFSv2 minus ERA5 considering 1979-2019 period.
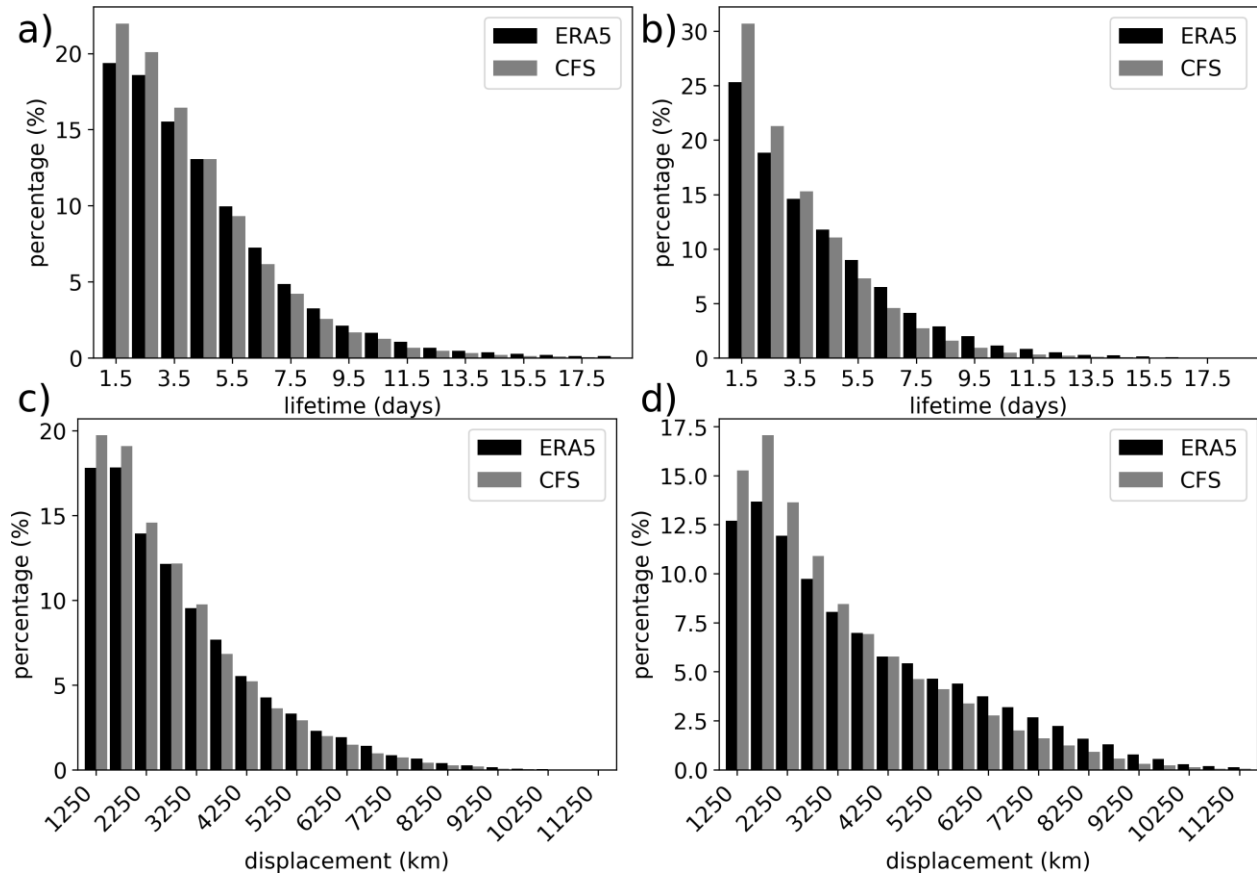
720

Figure 7 Histograms of cyclones (a,b) lifetime (days), and (c,d) displacement (km).for the (a,c) North Atlantic and (b,d) South Atlantic Oceans. The histograms were computed considering the whole 1979-2019 period for the ERA5 (black) and CFSR/CFSv2 (grey).
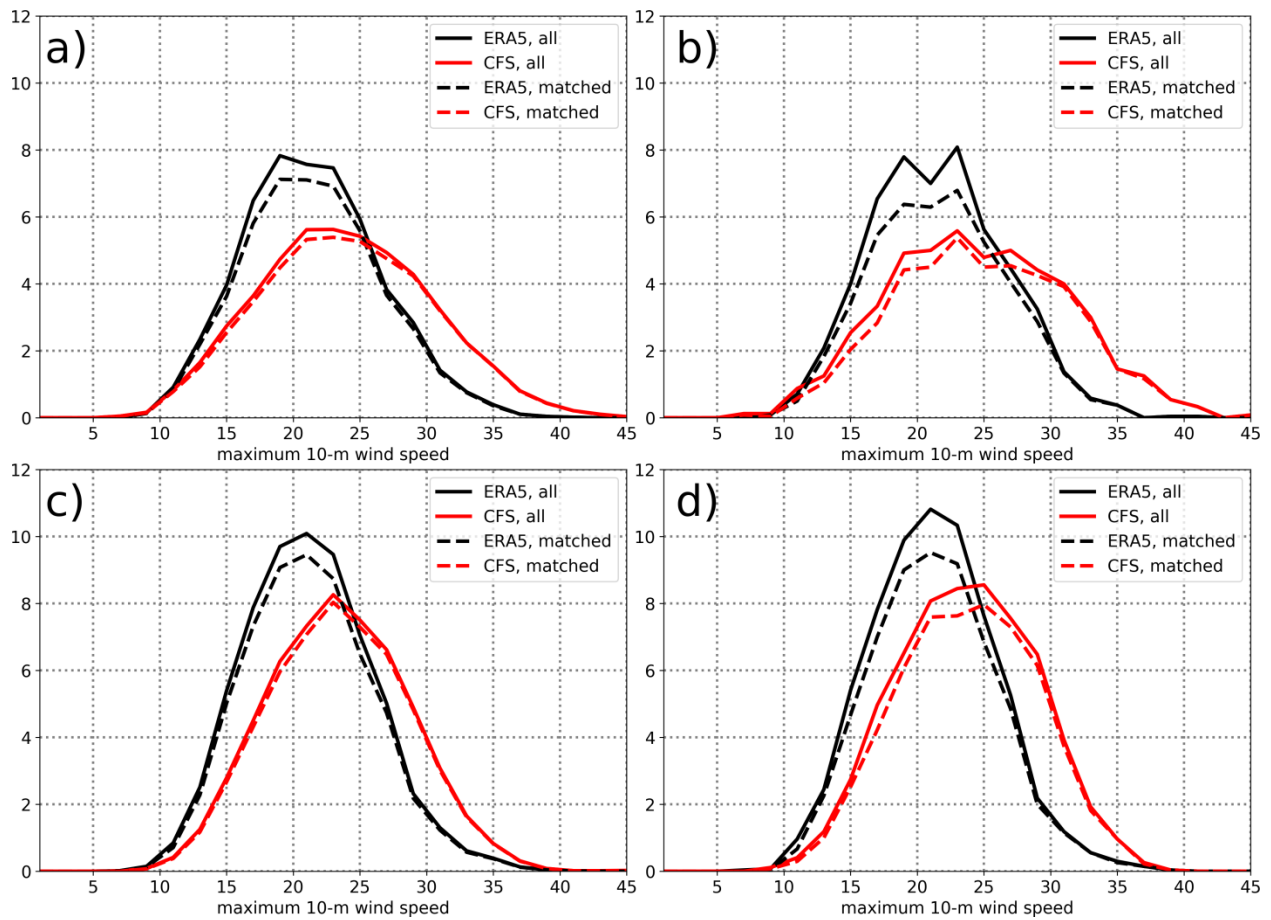
Figure 8. Cyclone's maximum 10-meters wind speed (m s^{-1}) distribution for the (a,b) North Atlantic in DJF, and (c,d) South Atlantic in JJA, considering the period between (a,c) 1979 and 2019, and (b,d) April/2011 and 2019. ERA5 distributions are in black, and CFSR/CFSv2 are in red. The dashed lines are the distributions computed for the matched cyclones in each dataset. The y-axis is cyclone per month.

721

41